Passive Doppler Synthetic Aperture Radar Imaging

Ling Wang
College of Information Science and Technology, Nanjing University of Aeronautics and Astronautics, Nanjing, 210016 China

Can Evren Yarman
Houston Technology Center, WesternGeco Schlumberger, Houston, TX 77042 USA

Birsen Yazıcı[1]
Department of Electrical, Computer and System Engineering, Rensselaer Polytechnic Institute, Troy, NY 12180 USA

Abstract

In this paper we consider passive airborne receivers that use backscattered signals from sources of opportunity transmitting fixed-frequency waveforms. Due to its combined passive synthetic aperture and the fixed-frequency nature of the transmitted waveforms, we refer to the system under consideration as Doppler Synthetic Aperture Hitchhiker (DSAH). We present a novel image formation method for DSAH. Our method first correlates the windowed signal obtained from one receiver with the windowed, filtered, scaled and translated version of the received signal from another receiver. This processing removes the transmitter related variables from the phase of the Fourier integral operator that maps the radiance of the scene to the correlated signal. We next use the microlocal analysis to reconstruct the scene radiance by the weighted-backprojection of the correlated signal. This imaging algorithm can put the visible edges of the scene radiance at the correct location, and under appropriate conditions, with correct strength. We show that the resolution of the image is directly related to the length of the support of the windowing function and the frequency of the transmitted waveform.

1 Introduction

In recent years, there has been a growing interest in passive radar applications using sources of opportunity [1–3]. This research effort is motivated by the growing availability of transmitters of opportunity, such as radio, television and cell phone stations, particularly in urban areas, as well as relatively low cost and rapid deployment of passive receivers.

While many of the passive radar applications are focused on the detection of airborne targets with ground based receivers recently, a number of methods for passive synthetic aperture radar has been developed. In [4], we reported a novel passive synthetic aperture imaging method that is based on the spatio-temporal correlation of the received signal and the filtered-backprojection technique. This method does not require receivers with high directivity or a priori knowledge about the transmitter locations and transmitted waveforms. The resolution analysis of the method shows that it is suitable for high-range-resolution waveforms, such as wideband pulses. However, most of the transmitters of opportunity, such as radio and TV stations, transmit single frequency waveforms. In this paper, we present a new passive synthetic aperture imaging method using sources of opportunity transmitting fixed-frequency waveforms. These waveforms are also referred to as high-Doppler-resolution or continuous-wave (CW) waveforms. Thus, we refer to the resulting method as the *Doppler Synthetic Aperture Hitchhiker* (DSAH) imaging method.

Our passive imaging method has the following advantages: (1) it does not require receivers with high directivity; (2) it can be used in the presence of both cooperative and non-cooperative sources of opportunity; (3) it can be used with stationary and/or mobile sources of opportunity; (4) it can be used with one or more airborne receivers; (5) it can be used under non-ideal imaging scenarios such as arbitrary flight trajectories and non-flat topography; (6) it has the desirable property of preserving the visible edges of the scene radiance in the reconstructed image. Additionally, it is an analytic image formation method that can be made computationally efficient.

The organization of our paper is as follows: In Section 2, we develop the forward model for DSAH and analyze the leading-order contributions to the windowed, filtered-scaled-and-correlated measurements. In Section 3, we develop a weighted-backprojection type image formation method for DSAH and analyze the underlying geometry and resolution of DSAH image formation.

2 DSAH Measurement Model

We use the following notational conventions throughout the paper. The bold Roman, bold italic and Roman lower-

case letters are used to denote variables in $\mathbb{R}^3$, $\mathbb{R}^2$ and $\mathbb{R}$, respectively, i.e., $\mathbf{z} = (z, z) \in \mathbb{R}^3$, with $z \in \mathbb{R}^2$ and $z \in \mathbb{R}$. The calligraphic letters ($\mathcal{F}, \mathcal{K}$ etc.) are used to denote operators.

We make the assumption that the earth's surface is located at a position given by $\mathbf{z} = (z, \psi(z)) \in \mathbb{R}^3$, where $z \in \mathbb{R}^2$ and $\psi : \mathbb{R}^2 \to \mathbb{R}$ is a known function for the ground topography. Furthermore, we assume that the scattering takes place in a thin region near the surface.

Under these assumptions, for a fixed-frequency waveform at frequency ω_0, given a pair of transmitter and receiver antennas located at $\mathbf{T}$ and $\mathbf{R}$ respectively, we model the received signal by [5]

$$f(t, \mathbf{R}, \mathbf{T}) \approx \int \frac{e^{-i\omega_0(t-(|\mathbf{R}-\mathbf{z}|+|\mathbf{z}-\mathbf{T}|)/c_0)}}{(4\pi)^2 |\mathbf{R}-\mathbf{z}||\mathbf{z}-\mathbf{T}|} \omega_0^2$$
$$\times J_{\mathrm{tr}}(\omega_0, \widehat{\mathbf{z}-\mathbf{T}}, \mathbf{T}) J_{\mathrm{rc}}(\omega_0, \widehat{\mathbf{z}-\mathbf{R}}, \mathbf{R}) \rho(z) \, dz \qquad (1)$$

where t denotes time, c_0 denotes the speed of light in free-space, $\rho(z)$ is the reflectivity function, and J_{tr} and J_{rc} are the transmitter and receiver antenna beam patterns, respectively. $\widehat{\mathbf{z}} = \mathbf{z}/|\mathbf{z}|$ denotes the unit vector in the direction of $\mathbf{z} \in \mathbb{R}^3$. For the rest of the paper, unless otherwise stated, we use $\mathbf{z} = \mathbf{z}(z) = (z, \psi(z))$.

We assume that there is a single, stationary transmitter of opportunity illuminating the scene. Let $\mathbf{T} \in \mathbb{R}^3$ denote the location of the transmitter and let there be N airborne receivers, each traversing a smooth trajectory $\boldsymbol{\gamma}_i(t)$, $i = 1, \cdots, N$ as shown in Figure 1.
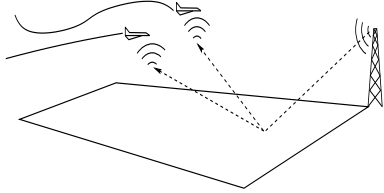

Figure 1: An illustration of the DSAH imaging geometry.

We define

$$s_i(t) = f(t, \boldsymbol{\gamma}_i(t), \mathbf{T}) \qquad (2)$$

as the received signal by the ith receiver, $i = 1, , \cdots, N$. Note that our imaging method is applicable to both mobile and stationary transmitter and also applicable to multiple transmitters and multiple transmit frequencies.

For a given point of interest z_0 on the ground topography and a fixed $\tau' \in \mathbb{R}$, we define the windowed, filtered-scaled-and-translated correlation of the received signals s_i and s_j by

$$c_{ij}^{\mathbf{z}_0}(\tau', \tau, \mu) = \int \frac{s_i(t+\tau') \, s_j^*(\mu t + \tau)}{B_{ij}(z_0, t, \tau', \tau, \mu)} \phi(t) \, |t| \, dt, \quad (3)$$

for some $\tau, \tau' \in \mathbb{R}$ and $\mu \in \mathbb{R}^+$, $i, j = 1, \cdots, N$, where $\phi(t)$ is a smooth compactly supported temporal windowing function centered at $t = 0$; and B_{ij} is a filter to be

determined later; and * denotes the complex conjugation. To simplify our notation, we drop the superscripts z_0 from $c_{ij}^{\mathbf{z}_0}(\tau', \tau, \mu)$ for the rest of our paper. Note that for a single receiver, we only have $c_{ij} = c_{11}$.

We make the incoherent-field approximation [6] by assuming that ρ and J_{tr} satisfy the following equalities:

$$C_\rho(\mathbf{z}, \mathbf{z}') = R_\rho(\mathbf{z})\delta(z - z'). \qquad (4)$$
$$C_{J_{\mathrm{tr}}}(\omega_0, \mathbf{z}, \mathbf{z}', \mathbf{T}) = R_T(\omega_0, \mathbf{z}, \mathbf{z}', \mathbf{T})\delta(z - z'). \qquad (5)$$

where C_ρ and $C_{J_{\mathrm{tr}}}$ denote the correlation function of ρ and J_{tr}, respectively. Note that R_ρ is the average power of the electromagnetic radiation emitted by the scene at location $\mathbf{z}$, and R_T is the average power of the electromagnetic radiation emitted by the transmitter at location $\mathbf{T}$ that is incident on the target surface at $\mathbf{z}$. In this regard, R_ρ is referred to as the *scene radiance* and R_T is referred to as the *transmitter irradiance* [6].

Substituting s_i and s_j into c_{ij}, under the assumption that ρ and J_{tr} are statistically independent, and using (4) and (5), we express the expectation of c_{ij} as follows:

$$E[c_{ij}(\tau', \tau, \mu)]$$
$$= \frac{\omega_0^4}{(4\pi)^4} \int e^{-i\omega_0(t+\tau'-(|\boldsymbol{\gamma}_i(t+\tau')-\mathbf{z}|+|\mathbf{T}-\mathbf{z}|)/c_0)}$$
$$\times e^{i\omega_0(\mu t+\tau-(|\boldsymbol{\gamma}_j(\mu t+\tau)-\mathbf{z}'|+|\mathbf{T}-\mathbf{z}'|)/c_0)}$$
$$\times \frac{R_T(\omega_0, \mathbf{z}, \mathbf{z}', \mathbf{T}) A_{R_{ij}}(\omega_0, \mathbf{z}, \mathbf{z}', t, \tau', \tau, \mu)}{G_{ij}(\mathbf{z}, \mathbf{z}', t, \tau', \tau, \mu) \, B_{ij}(\mathbf{z}_0, t, \tau', \tau, \mu)}$$
$$\times R_\rho(\mathbf{z})\delta(z-z')dz\,dz' \, \phi(t) \, |t| \, dt \qquad (6)$$

where $A_{R_{ij}}$ is the product of the receiver antenna beam patterns,

$$A_{R_{ij}}(\omega_0, \mathbf{z}, \mathbf{z}', t, \tau', \tau, \mu)$$
$$= J_{\mathrm{rc}}(\omega_0, \mathbf{z} - \widehat{\boldsymbol{\gamma}_i(t+\tau')}, \boldsymbol{\gamma}_i(t+\tau'))$$
$$\times J_{\mathrm{rc}}^*(\omega_0, \mathbf{z}' - \widehat{\boldsymbol{\gamma}_j(\mu t + \tau)}, \boldsymbol{\gamma}_j(\mu t + \tau)) \qquad (7)$$

and G_{ij} is the product of the geometric spreading factors,

$$G_{ij}(\mathbf{z}, \mathbf{z}', t, \tau', \tau, \mu) = |\mathbf{T} - \mathbf{z}| \, |\mathbf{T} - \mathbf{z}'| \qquad (8)$$
$$\times |\boldsymbol{\gamma}_i(t+\tau') - \mathbf{z}| \, |\boldsymbol{\gamma}_j(\mu t + \tau) - \mathbf{z}'|. \qquad (9)$$

Note that for non-cooperative sources of opportunity, $\mathbf{T}$ and thus $|\mathbf{T} - \mathbf{z}| \, |\mathbf{T} - \mathbf{z}'|$, are unknown.

Now using the Taylor series expansion of $|\boldsymbol{\gamma}_i(t+\tau') - \mathbf{z}|$ and $|\boldsymbol{\gamma}_j(\mu t + \tau) - \mathbf{z}'|$ at $t = 0$, substituting the approximations back into (6), and performing the $\mathbf{z}'$ integration, we have

$$E[c_{ij}(\tau', \tau, \mu)] \approx \mathcal{F}_{ij}[R_\rho](\tau, \mu)$$
$$= \int e^{-i\varphi_{ij}(t, \mathbf{z}, \tau', \tau, \mu)} \frac{A_{ij}(\mathbf{z}, t, \tau', \tau, \mu)}{B_{ij}(\mathbf{z}_0, t, \tau', \tau, \mu)} R_\rho(\mathbf{z}) \, d\mathbf{z} \, |t| \, dt \qquad (10)$$

where

$$\varphi_{ij}(t, \mathbf{z}, \tau', \tau, \mu) =$$
$$\omega_0 t [1 - (\widehat{\boldsymbol{\gamma}_j(\tau) - \mathbf{z}}) \cdot \dot{\boldsymbol{\gamma}}_j(\tau)/c_0] [S_{ij}(\tau', \tau, \mathbf{z}) - \mu] \qquad (11)$$

with

$$S_{ij}(\tau', \tau, \mathbf{z}) = \frac{1 - (\widehat{\boldsymbol{\gamma}_i(\tau') - \mathbf{z}}) \cdot \dot{\boldsymbol{\gamma}}_i(\tau')/c_0}{1 - (\widehat{\boldsymbol{\gamma}_j(\tau) - \mathbf{z}}) \cdot \dot{\boldsymbol{\gamma}}_j(\tau)/c_0} \qquad (12)$$

and

$$A_{ij}(\mathbf{z}, t, \tau', \tau, \mu) = \frac{\tilde{R}_T(\omega_0, \mathbf{z}) A_{R_{ij}}(\omega_0, \mathbf{z}, \mathbf{z}, t, \tau', \tau, \mu)}{G_{ij}(\mathbf{z}, \mathbf{z}, t, \tau', \tau, \mu)}$$

$$\times \frac{\omega_0^4 \phi(t)}{(4\pi)^4} \mathrm{e}^{-\mathrm{i}\omega_0(\tau' - \tau - (|\boldsymbol{\gamma}_i(\tau') - \mathbf{z}| - |\boldsymbol{\gamma}_j(\tau) - \mathbf{z}|)/c_0)} \qquad (13)$$

with $\tilde{R}_T(\omega_0, \mathbf{z}) = R_T(\omega_0, \mathbf{z}, \mathbf{z}, \mathbf{T})$. We refer to $S_{ij}(\tau', \tau, \mathbf{z})$ as the *Doppler-hitchhiker-scale-factor*, and φ_{ij} and A_{ij}/B_{ij} as the phase and amplitude terms of the linear operator $\mathcal{F}_{ij}$.

For cooperative sources of opportunity, $\tilde{R}_T(\omega_0, \mathbf{z})$ in (13) is replaced with $J_{\mathrm{tr}}(\omega_0, \widehat{\mathbf{z} - \mathbf{T}}, \mathbf{T})J_{\mathrm{tr}}^*(\omega_0, \widehat{\mathbf{z}' - \mathbf{T}}, \mathbf{T})$.

Note that the filtered-scaled-and-translated correlation of the received signal removes all transmitter related terms from the phase of the operator $\mathcal{F}_{ij}$.

We assume that for some m_A, A_{ij}/B_{ij} satisfies the following inequality:

$$\sup_{(t,\mu,\tau,\mathbf{z}) \in \mathcal{U}} \left| \partial_t^{\alpha_t} \partial_\mu^{\alpha_\mu} \partial_\tau^\beta \partial_{z_1}^{\epsilon_1} \partial_{z_2}^{\epsilon_2} \frac{A_{ij}(\mathbf{z}, t, \tau', \tau, \mu)}{B_{ij}(\mathbf{z}_0, t, \tau', \tau, \mu)} |t| \right|$$

$$\leq C_A (1 + t^2)^{(m_A - |\alpha_t|)/2} \qquad (14)$$

where $\mathcal{U}$ is any compact subset of $\mathbb{R}^+ \times \mathbb{R}^+ \times \mathbb{R} \times \mathbb{R} \times \mathbb{R}^2$, and the constant C_A depends on $\mathcal{U}, \alpha_{t,\mu}, \beta, \epsilon_{1,2}$. This assumption is needed in order to make various stationary phase calculations hold. Under the assumption (14), (10) defines $\mathcal{F}$ as a *Fourier integral operator* whose leading order contributions come from those points lying in the intersection of the illuminated surface $(\mathbf{z}, \boldsymbol{\psi}(\mathbf{z}))$ and points that have the same Doppler-hitchhiker-scale-factor, i.e., $\{\mathbf{z} \in \mathbb{R}^3 : S_{ij}(\tau', \tau, \mathbf{z}) = \mu\}$.

3 Image Formation

We form an image of the scene radiance by the superposition of the weighted and backprojected data, $E[c_{ij}(\tau, \mu)]$ as follows:

$$\tilde{R}_\rho(\mathbf{z}) = \sum_{ij} \int \mathcal{K}_{ij}[E[c_{ij}]](\mathbf{z}, \tau') d\tau'$$

where

$$\mathcal{K}_{ij}[E[c_{ij}]](\mathbf{z}, \tau') = \int \mathrm{e}^{\mathrm{i}\varphi_{ij}(t, \mathbf{z}, \tau', \tau, \mu)} Q_{ij}(\mathbf{z}, \tau', \tau, \mu)$$

$$\times E[c_{ij}(\tau', \tau, \mu)] dt d\tau d\mu. \qquad (15)$$

We refer to $\mathcal{K}_{ij}$ as the weighted-backprojection operator with respect to the ith and jth receivers with weight Q_{ij} to be determined below.

We rewrite $\tilde{R}_\rho$ as

$$\tilde{R}_\rho(\mathbf{z}) = \sum_{ij} \mathcal{K}_{ij}\mathcal{F}_{ij}[R_\rho](\mathbf{z}) = \int L(\mathbf{z}, \mathbf{z}')R_\rho(\mathbf{z}') d\mathbf{z}' \quad (16)$$

where $L(\mathbf{z}, \mathbf{z}')$ is the *point spread function* (PSF) of the imaging operator given by

$$L(\mathbf{z}, \mathbf{z}') = \sum_{ij} \int L_{ij}(\mathbf{z}, \mathbf{z}', \tau')d\tau' \qquad (17)$$

and

$$L_{ij}(\mathbf{z}, \mathbf{z}', \tau') = \int \mathrm{e}^{\mathrm{i}[\varphi_{ij}(t, \mathbf{z}, \tau', \tau, \mu) - \varphi_{ij}(t', \mathbf{z}', \tau', \tau, \mu)]}$$

$$\times Q_{ij}(\mathbf{z}, \tau', \tau, \mu) \frac{A_{ij}(\mathbf{z}', t, \tau', \tau, \mu)}{B_{ij}(\mathbf{z}, t, \tau', \tau, \mu)} |t| dt' dt d\tau d\mu. \quad (18)$$

Using the stationary phase theorem [7] to approximate the t' and μ integrations, we obtain

$$L_{ij}(\mathbf{z}, \mathbf{z}', \tau') \approx$$
$$\int \mathrm{e}^{-\mathrm{i}\omega_0 t[1 - (\widehat{\boldsymbol{\gamma}_j(\tau) - \mathbf{z}}) \cdot \dot{\boldsymbol{\gamma}}_j(\tau)/c_0][S_{ij}(\tau', \tau, \mathbf{z}') - S_{ij}(\tau', \tau, \mathbf{z})]}$$

$$\times Q_{ij}(\mathbf{z}, \tau', \tau) \frac{A_{ij}(\mathbf{z}', t, \tau', \tau)}{B_{ij}(\mathbf{z}, t, \tau', \tau)} |t| dt d\tau.$$

Applying the method of stationary phase to the t and τ integrals, we see that the main contribution to $L_{ij}(\mathbf{z}, \mathbf{z}', \tau')$ comes from those critical points of its phase that satisfy the conditions:

$$S_{ij}(\tau', \tau, \mathbf{z}') = S_{ij}(\tau', \tau, \mathbf{z}), \qquad (19)$$

and

$$a_j^\Sigma(\tau, \mathbf{z})/[1 - (\widehat{\boldsymbol{\gamma}_j(\tau) - \mathbf{z}}) \cdot \dot{\boldsymbol{\gamma}}_j(\tau)/c_0] =$$
$$a_j^\Sigma(\tau, \mathbf{z}')/[1 - (\widehat{\boldsymbol{\gamma}_j(\tau) - \mathbf{z}'}) \cdot \dot{\boldsymbol{\gamma}}_j(\tau)/c_0] \qquad (20)$$

where

$$a_j^\Sigma(\tau, \mathbf{z}) = \frac{1}{|\boldsymbol{\gamma}_j(\tau) - \mathbf{z}|}$$
$$\times [\dot{\boldsymbol{\gamma}}_{j,\perp}(\tau, \mathbf{z}) \cdot \dot{\boldsymbol{\gamma}}_j(\tau)]^2 + (\widehat{\boldsymbol{\gamma}_j(\tau) - \mathbf{z}}) \cdot \ddot{\boldsymbol{\gamma}}_j(\tau) \quad (21)$$

Note that $\dot{\boldsymbol{\gamma}}_{j,\perp}(\tau, \mathbf{z})$ is the projection of the receiver velocity $\dot{\boldsymbol{\gamma}}_j(\tau)$ onto the plane whose normal direction is along $\widehat{\boldsymbol{\gamma}_j(\tau) - \mathbf{z}}$ and $a_j^\Sigma(\tau, \mathbf{z})$ is the total relative radial acceleration of the jth receiver in the direction of $\widehat{\boldsymbol{\gamma}_j(\tau) - \mathbf{z}}$.

We define

$$f_j(\tau, \mathbf{z}) := a_j^\Sigma(\tau, \mathbf{z})/[1 - (\widehat{\boldsymbol{\gamma}_j(\tau) - \mathbf{z}}) \cdot \dot{\boldsymbol{\gamma}}_j(\tau)/c_0] \quad (22)$$

and refer to $f_j(\tau, \mathbf{z})$ as the *DSAH Doppler-rate* of the jth receiver. The critical points $\mathbf{z}$ of the phase of $L_{ij}(\mathbf{z}, \mathbf{z}', \tau')$ are those points that have the same Doppler-hitchhiker-scale-factor and DSAH Doppler-rate with $\mathbf{z}'$. We assume that the only critical point within the region of interest is $\mathbf{z} = \mathbf{z}'$.

To determine the weight and the filter, we linearize $S_{ij}(\tau', \tau, \mathbf{z}')$ around $\mathbf{z}' = \mathbf{z}$ to write

$$
\begin{aligned}
L_{ij}(\mathbf{z}, \mathbf{z}', \tau') \quad &= \int \mathrm{e}^{-\mathrm{i}\, t\, \boldsymbol{\Xi}_{ij}(\tau',\tau,\mathbf{z})\cdot(\mathbf{z}'-\mathbf{z})}\, Q_{ij}(\mathbf{z}, \tau', \tau) \\
&\times \tfrac{A_{ij}(\mathbf{z},t,\tau',\tau)}{B_{ij}(\mathbf{z},t,\tau',\tau)}\, |t|\, dt\, d\tau \quad (23)
\end{aligned}
$$

where

$$
\begin{aligned}
\boldsymbol{\Xi}_{ij}(\tau', \tau, \mathbf{z}) = \omega_0 [1 - (\widehat{\boldsymbol{\gamma}_j(\tau) - \mathbf{z}}) \cdot \dot{\boldsymbol{\gamma}}_j(\tau)/c_0] \\
\times \nabla_{\mathbf{z}} S_{ij}(\tau', \tau, \mathbf{z}). \quad (24)
\end{aligned}
$$

In (23) for each τ' and $\mathbf{z}$, we make the following change of variables:

$$
(t, \tau) \rightarrow \boldsymbol{\xi}_{ij} = t\, \boldsymbol{\Xi}_{ij}(\tau', \tau, \mathbf{z}) \quad (25)
$$

and we choose the weight and the filter as follows:

$$
\begin{aligned}
Q_{ij}(\mathbf{z}, \tau', \tau) &= \left[|t| \left| \frac{\partial(t, \tau)}{\partial \boldsymbol{\xi}_{ij}} \right| \right]^{-1} \\
&= \left| \det \left[\begin{array}{c} \boldsymbol{\Xi}_{ij}(\tau', \tau, \mathbf{z}) \\ \partial_\tau \boldsymbol{\Xi}_{ij}(\tau', \tau, \mathbf{z}) \end{array} \right] \right| \quad (26)
\end{aligned}
$$

and

$$
\begin{aligned}
B_{ij}(\mathbf{z}, t, \tau', \tau, \mu) &= \chi_{\Omega_{ij,\tau',\mathbf{z}}}(\mathbf{z}, t, \tau', \tau) \\
&\times A_{ij}(\mathbf{z}, t, \tau', \tau, \mu) \quad (27)
\end{aligned}
$$

where $\chi_{\Omega_{ij,\tau',\mathbf{z}}}$ is a smooth cut-off function equal to one in the interior of $\Omega_{ij,\tau',\mathbf{z}}$ and zero in the exterior of $\Omega_{ij,\tau',\mathbf{z}}$. We refer to $\Omega_{ij,\tau',\mathbf{z}}$ as the *partial data collection manifold* at $(\tau', \mathbf{z})$ obtained by the ith and jth receivers for a fixed τ' and refer to the union $\cup_{ij,\tau'} \Omega_{ij,\tau',\mathbf{z}}$ as the *data collection manifold* at $\mathbf{z}$ and denote it by $\Omega_{\mathbf{z}}$. This set determines many of the properties of the image.

Note that we choose the filter to compensate for the terms involving antenna beam patterns and geometric spreading functions and the weight to perform proper interpolation in the phase space going from (t, τ) to $\boldsymbol{\xi}_{ij}$ coordinates. These choices make the leading order term of $L_{ij}(\mathbf{z}, \mathbf{z}', \tau')$ in (23) to be the Dirac-delta function. Substituting (25), (26) and (27) into (16), we obtain

$$
\begin{aligned}
\tilde{R}_\rho(\mathbf{z}) &= \sum_{ij} \mathcal{K}_{ij}[\mathcal{F}_{ij}[R_\rho]](\mathbf{z}) \\
&\approx \sum_{ij} \int_{\Omega_{ij,\tau',\mathbf{z}}} \mathrm{e}^{-\mathrm{i}\boldsymbol{\xi}_{ij}\cdot(\mathbf{z}'-\mathbf{z})} R_\rho(\mathbf{z}')\, d\mathbf{z}'\, d\boldsymbol{\xi}_{ij}\, d\tau'. \quad (28)
\end{aligned}
$$

(28) shows that the image $\tilde{R}_\rho$ is a band-limited version of R_ρ whose band-width is determined by the data collection manifold $\Omega_{\mathbf{z}}$, which describes the resolution of the reconstructed image $\tilde{R}_\rho$ at $\mathbf{z}$. The larger the data collection manifold, the better the resolution of the image is. With the choice of the weight and filter given in (26) and (27), respectively, the resulting image formation algorithm recovers the visible edges of the scene radiance not only at the right location and orientation, but also at the right strength. Microlocal analysis of (28) tell us that an edge at point $\mathbf{z}$ is visible if the direction $\mathbf{n}_{\mathbf{z}}$ normal to the edge is contained in $\Omega_{\mathbf{z}}$ [8]. Consequently, an edge at point $\mathbf{z}$ with $\mathbf{n}_{\mathbf{z}}$ normal to edge is visible if there exists i, j, τ', τ such that $\boldsymbol{\xi}_{ij}$

is parallel to $\mathbf{n}_{\mathbf{z}}$. Furthermore, the band-width contribution of $\boldsymbol{\xi}_{ij} = t\boldsymbol{\Xi}_{ij}(\tau', \tau, \mathbf{z})$ to a visible edge at $\mathbf{z}$ is given by $L_\phi |\boldsymbol{\Xi}_{ij}(\tau', \tau, \mathbf{z})|$ where L_ϕ denotes the length of the support of $\phi(t)$. Thus, longer the support of $\phi(t)$, larger the magnitude of $\boldsymbol{\xi}_{ij}$ becomes, giving rise to sharper reconstructed edges perpendicular to $\boldsymbol{\xi}_{ij}$, $i, j = 1, \ldots, N$. Additionally, higher the ω_0, the frequency of the transmitted signal, larger the magnitude of $\boldsymbol{\xi}_{ij}$ becomes, contributing to higher image resolution.

4 Conclusion

In this paper, we developed a novel image formation method for passive SAR that uses transmitters of opportunity with fixed-frequency waveforms. The method is based on the windowed, filtered-scaled-and-translated correlation of the received signals at different (or the same) receiver and weighted-backprojection of the resulting correlated signal. The analysis of the point spread function of the imaging operator shows that the weighted-backprojection algorithm puts the visible edges of the scene radiance at the correct location, and under appropriate conditions, with correct strength. We will present the simulation results of this imaging method on the conference.

References

[1] H. D. Griffiths and C. J. Baker, "Passive coherent location radar systems. part 1: Performance prediction," *IEE Proc.-Radar Sonar Navig.*, vol. 152, no. 3, June 2005.

[2] D. Poullin, "Passive detection using digital broadcasters (DAB, DVB) with COFDM modulation," *IEE Proc.-Radar Sonar Navig.*, vol. 152, no. 3, pp. 143–152, June 2005.

[3] R. Pollard, "The role of passive radar sensors for air traffic control," in *The Institution of Engineering and Technology Seminar on the Future of Civil Radar*, 2006.

[4] C.E. Yarman and B. Yazıcı, "Synthetic aperture hitch-hiker imaging," *IEEE Transactions on Imaging Processing*, vol. 17, no. 11, pp. 2156–2173, Nov. 2008.

[5] C.J. Nolan and M. Cheney, "Synthetic aperture inversion for arbitrary flight paths and non-flat topography," *IEEE Transactions on Image Processing*, vol. 12, pp. 1035–1043, 2003.

[6] H.H. Barrett and K.J. Myers, *Foundations of image science*, Wiley-Interscience, Hoboken, NJ, 2004.

[7] N. Bleistein and R.A. Handelsman, *Asymptotic Expansions of Integrals*, Dover, New York, 1986.

[8] C. J. Nolan and M. Cheney, "Synthetic aperture inversion," *Inverse Problems*, vol. 18, pp. 221–236, 2002.